Eur. Phys. J. A **16**, 139–147 (2003)
DOI 10.1140/epja/i2002-10067-y

THE EUROPEAN PHYSICAL JOURNAL A

Beta-neutrino angular correlation in the decay of ^{14}O

Scalar coupling and interatomic interaction

V. Vorobel[5,a], Ch. Briançon[4], V. Brudanin[1], V. Egorov[1], J. Deutsch[2], R. Prieels[2], N. Severijns[2,3], Yu. Shitov[1], Ch. Vieu[2], Ts. Vylov[1], I. Yutlandov[1], and Sh. Zaparov[1]

[1] Joint Institute for Nuclear Research, 141980 Dubna, Russia
[2] Université Catholique de Louvain, B-1348 Louvain-la-Neuve, Belgium
[3] Katholieke Universiteit Leuven, B-3001 Leuven, Belgium
[4] Centre de Spectrométrie Nucléaire et de Spectrométrie de Masse, 91405 Orsay, France
[5] Faculty of Mathematics and Physics, Charles University, Prague, Czech Republic

Received: 21 May 2002 / Revised version: 02 July 2002 /
Published online: 17 January 2003 –
Communicated by J. Äystö

Abstract. The positrons and coincident gamma-rays following the pure Fermi $0^+ \to 0^+$ branch of β^+-decay in ^{14}O were measured. The Doppler shift of the γ-quantum observed is sensitive to the beta-neutrino correlation coefficient, which is unity ($\alpha = 1$) in the absence of scalar coupling. The interatomic interaction of recoiling daughters was noticed, which has prevented to obtain an improved result for scalar coupling despite of the excellent statistical accuracy of the measurement. At the same time, it was shown that the method described can be used as a very sensitive and flexible tool to probe the interatomic interactions in matter at the hundred eV energy level. Perspectives in this direction as well as the future angular-correlation experiments aimed to search for scalar coupling in beta-decay are discussed.

PACS. 13.10.+q Weak and electromagnetic interactions of leptons – 23.20.En Angular distribution and correlation measurements – 23.40.Bw Weak-interaction and lepton (including neutrino) aspects – 25.75.Gz Particle correlations

1 Introduction

Searching for effects beyond the Standard Model (SM) is in the mainstream of modern physics. Here we concentrate on investigations of weak couplings in beta-decay. In addition to the dominant V-A weak current, the admixture of scalar (S) and tensor (T) interactions is allowed in most theoretical extensions of SM. According to former experimental data in the semileptonic sector of beta-decay the presence of S- and T-couplings cannot be excluded at a level of 6% (68% CL) [1] and 9% (95% CL) [2], respectively[1]. Rather strong disagreement between experimental data and SM-based theoretical predictions was recently obtained by our group investigating ordinary muon capture on ^{16}O [4][2]. The admixture of S-coupling is considered as a possible reason of this discrepancy. Therefore, more accurate experiments are called for in order to clarify this intriguing situation.

Let us recall that the measurement of angular correlations is *the most sensitive*, direct method to investigate weak couplings[3]. As a consequence, we started a set of measurements of beta-neutrino correlation in beta-decay.

By measuring the beta-decay of ^{18}Ne, we already illustrated the applicability of our method [5], which *differs* from the other ones. The poor precision of the result (29% upper limit for S-interaction) was due to the low statistics (5.3×10^3 events).

Investigating the beta-decay of ^{14}O, we improved our technique significantly collecting $\sim 2 \times 10^6$ useful events. Unfortunately, it turned out to be difficult to extract a better result for scalar couplings using this huge amount of data. Studying the beta-decay of this specific nucleus, we encountered an unexpectedly strong interatomic interaction of the recoiling daughter nuclei (10%–15% of the effect observed). This interaction introduces a large systematic error, which is difficult to take into account precisely.

[a] e-mail: vorobel@ipnp.troja.mff.cuni.cz

[1] The recent inclusion of radiative corrections modifies the limit for T-couplings up to 18% [3].

[2] This experiment in the muon sector has similar purposes than the ones undertaken here in the field of beta-decay.

[3] In fact, even the names of weak constants were given according to the angular behaviours of the corresponding weak terms (vector, scalar, etc.) emphasizing the basic role of these characteristics.

Nevertheless, looking at the problem from the opposite side, one can conclude that some beta-neutrino angular correlations in beta-decay are very sensitive to the interatomic interaction in matter. As a result, these effects can be used as a probe of interatomic forces in solids or in molecules of gases or liquids. We, therefore, considered it important to expose here our experiment and its results being confident that this technique can be used as a tool for solid state or molecular studies as well as in astrophysics.

Future experiments, which are planned to search for scalar coupling in beta-neutrino angular correlation, are also discussed.

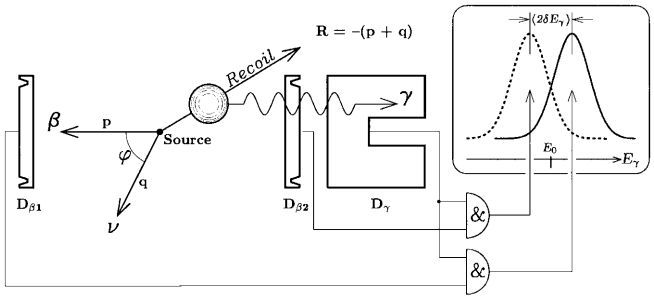

Fig. 1. The principle of measurement of beta-neutrino angular correlation.

2 Theory

In this section we present the basic theoretical concepts, motivations and principles of β-ν correlation investigations as well as our interpretation of the interatomic effect we observed.

2.1 Beta-neutrino angular correlation

The angular distribution between the momenta of the β-particle $\mathbf{p}$ and of the neutrino $\mathbf{q}$ emitted in β-decay from unpolarized nuclei is described by the correlation function

$$W(\varphi) = 1 + \alpha \frac{(\mathbf{p} \cdot \mathbf{q})}{W_\beta \cdot W_\nu} = 1 + \alpha \frac{v_\beta}{c} \cos(\varphi), \qquad (1)$$

W_β and W_ν being the total energy of the β-particle and of the neutrino, respectively; φ is the angle between the momenta of these particles and v_β/c the velocity of the β-particle relative to the speed of light. The Fierz interference term is neglected, assuming $C'_S + C_S = 0$ [6]. In the case of pure Fermi transitions as the one investigated in the current project, the angular-correlation coefficient α depends only on vector C_V, C'_V and scalar C_S, C'_S couplings:

$$\alpha = \frac{|C_V|^2 + |C'_V|^2 - |C_S|^2 - |C'_S|^2}{|C_V|^2 + |C'_V|^2 + |C_S|^2 + |C'_S|^2}\,. \qquad (2)$$

A deviation of α from unity would indicate the admixture of scalar coupling.

Measuring the kinematics of the products of a superallowed pure Fermi $0^+ \rightarrow 0^+$ beta-transition allows to determine the correlation coefficient α experimentally. The momentum of the β-particle $\mathbf{p}$ is usually registered directly, while the neutrino energy is fixed by conservation of energy[4]

$$W_\nu = qc = T^0_\beta - T_\beta, \qquad (3)$$

where T^0_β is the end point (maximal kinetic energy) of the beta-spectrum and T_β is the kinetic energy of the emitted β-particle. The neutrino momentum $\mathbf{q}$ can, however, only be determined indirectly, by detecting the recoiling daughter nucleus (momentum $\mathbf{R}$)

$$\mathbf{R} = -(\mathbf{p} + \mathbf{q}). \qquad (4)$$

The direct measurements of the recoils are rather difficult due to their low energies (typically about 10–100 eV), although various experimental techniques were developed for this purpose. If, however, the daughter nucleus produced in the beta-decay is in an excited state and the half-life of this excited state is short enough, the Doppler shift of the emitted γ-quantum (momentum $\mathbf{k}$) can be detected, instead

$$\delta E_\gamma = E_\gamma - E^0_\gamma = E^0_\gamma \cdot \frac{(\mathbf{R} \cdot \mathbf{k})}{M \cdot c \cdot k}\,, \qquad (5)$$

where M is the mass of the daughter nucleus and a non-relativistic approximation is used. The precise measurement of the energy shift of the Doppler-shifted γ-rays, δE_γ, in coincidence with β-particles, allows then to determine the full kinematics of the investigated beta-decay, including the neutrino momentum [7].

As the value of δE_γ is too small (typically several hundreds of eV) in comparison with the energy resolution of a γ detector (keV level) we measure *the average Doppler shift* of the gamma-line following the β-decay and emitted at some angle θ relatively to $\mathbf{p}$. Integrating (5) over the neutrinos emitted according to the distribution (1) and taking into account (3)-(4) one can see, that this observable is sensitive to the momentum of the β-particle as well as to the correlation coefficient α:

$$\langle \delta E_\gamma \rangle_\nu = f(T_\beta, \alpha). \qquad (6)$$

The principle of the measurement is shown in fig. 1. The beta-particles are detected by the energy-sensitive detectors $D_{\beta 1}$ and $D_{\beta 2}$ mounted inside the vacuum chamber at opposite directions relative to the source. Coincident gamma-rays following beta-decay are observed with the detector D_γ located outside the vacuum chamber at $\theta = 0^\circ$ or 180°. In this case and with an ideal point-like source and detectors, the function (6) takes the simple

[4] Here we assume a massless neutrino and neglect the recoils energy for simplicity.

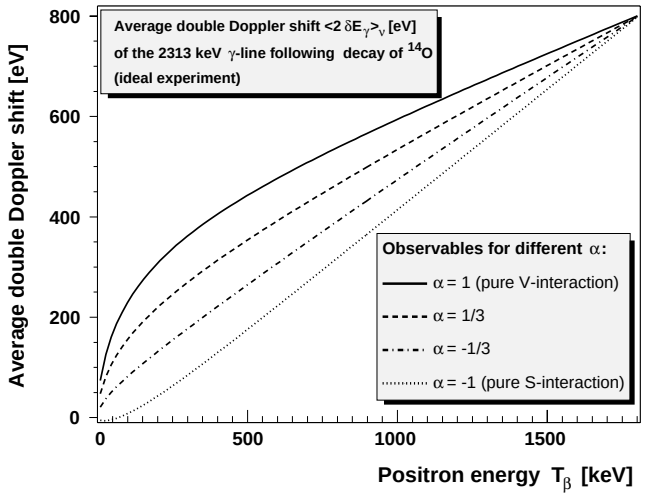

Fig. 2. Theoretical Doppler-shift $\langle 2\delta E_\gamma \rangle_\nu$ curves calculated for different values of the correlation coefficient α. The coefficient α has values 1, 1/3, $-1/3$, -1 for pure V, T, A, S type of interactions, respectively. The curves were calculated accordingly to eq. (7) for the observed transition ($0^+ \to 0^+$ β^+-decay branch of ^{14}O) in an ideal setup geometry with point-like source and detectors located opposite to the source (see fig. 1).

form

$$\frac{\langle \delta E_\gamma \rangle_\nu}{E_\gamma^0} = \pm \frac{p}{Mc}\left(1 + \frac{\alpha}{3}\frac{q}{m_e c}\right) = \pm \frac{\sqrt{T_\beta(T_\beta + 2m_e c^2)}}{Mc^2}\left(1 + \frac{\alpha}{3}\frac{T_\beta^0 - T_\beta}{m_e c^2}\right), \quad (7)$$

where the sign is either positive for oppositely moving beta-particle and γ-quantum ($D_\gamma \cdot D_{\beta 1}$ coincidence) or negative otherwise ($D_\gamma \cdot D_{\beta 2}$ coincidence). Average theoretical (doubled) Doppler-shift curves have been calculated according to eq. (7), M being the mass of ^{14}N, for several α-values, and are presented in fig. 2.

The emitted γ-quanta are sorted in two energy spectra $E_\gamma(D_\gamma \cdot D_{\beta 1})$ or $E_\gamma(D_\gamma \cdot D_{\beta 2})$ depending on the beta detector activated. As a result, the two γ-peaks which are measured *simultaneously*[5], will present a mean γ energy differing by the average double Doppler shift. Recording the beta-particle energy, one obtains in addition the measured Doppler shift as a function of the beta-particle energy. Fitting this experimental curve with the theoretical functions (fig. 2) allows to evaluate the correlation coefficient α.

2.2 Interatomic interactions

The interaction of the recoiling nucleus with the material of the source attenuates the correlation. The attenuation factor will depend on the lifetime of the recoiling excited state. Other important features are the chemical and physical properties of the source and of the daughter atoms; *e.g.*, the interatomic interaction is very strong in solid targets, where the recoils are moving in a lattice, and becomes negligible in the case of a chemically inactive daughter nucleus and in gaseous sources if the lifetime is short enough.

[5] As it was explained in ref. [5], this method allows to eliminate many systematic errors which could appear otherwise in sequential measurements.

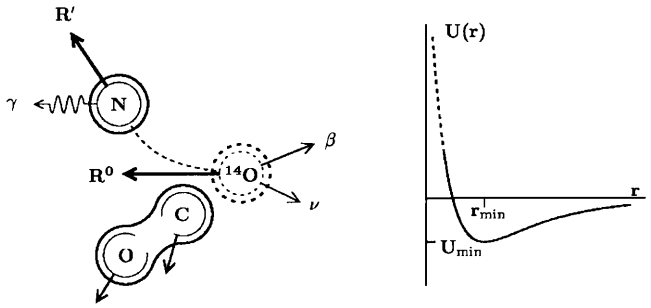

Fig. 3. The interaction of the recoil atom (ion) with the rest of the CO_2 molecule illustrates the principle of interatomic effect which changes the initial momentum R^0 of the recoiling daughter nucleus to R' at the moment of the γ emission.

In the current experiment ^{14}O was an atom of the CO_2 molecule, as it was determined in an auxiliary experiment. In this experiment the produced ^{14}O was trapped in chemicals selective to various molecular forms and monitored with a Ge detector. After beta-decay, the recoiling ^{14}N atom interacts with the rest of the molecule before emitting the γ-quantum (see fig. 3). Because of the ensuing change of the ^{14}N momentum from R^0 to R', the Doppler shift observed (eq. (5)) differs from the one caused by beta-decay. To measure the real correlation we must observe gamma-rays emitted by daughter nuclei which did not change their momentum after the beta-decay by interatomic interactions.

In the present case a complicated set of molecular and atomic processes is triggered by the beta-decay. Beta-decay changes the charge of the nucleus. The energy and momentum release is partially transferred to the atoms. Both effects force electromagnetic perturbations in the O-C-N system (the shaking, reconstruction and breaking of electron orbits). This dynamic picture is not well understood yet and is studied in "hot" chemistry, thermonuclear physics, etc.

As the recoils are non-relativistic, one can use the simple model of two particles (^{14}N atom and the remaining (CO) complex) moving in a classical interatomic potential. We restrict ourselves to this rough approximation just to illustrate the sensitivity of our observables to this interatomic potential. However, the experimental data can be re-analysed in the frame of any other, more precise and complete model of interatomic interactions.

The potential-energy dependence on the ^{14}N-(CO) distance r, known as Lennard-Jones formula, was chosen for our purposes

$$U_{\mathrm{LJ}}(r) = -U_{\min}\left\{\left(\frac{r_{\min}}{r}\right)^{12} - 2\left(\frac{r_{\min}}{r}\right)^{6}\right\}. \quad (8)$$

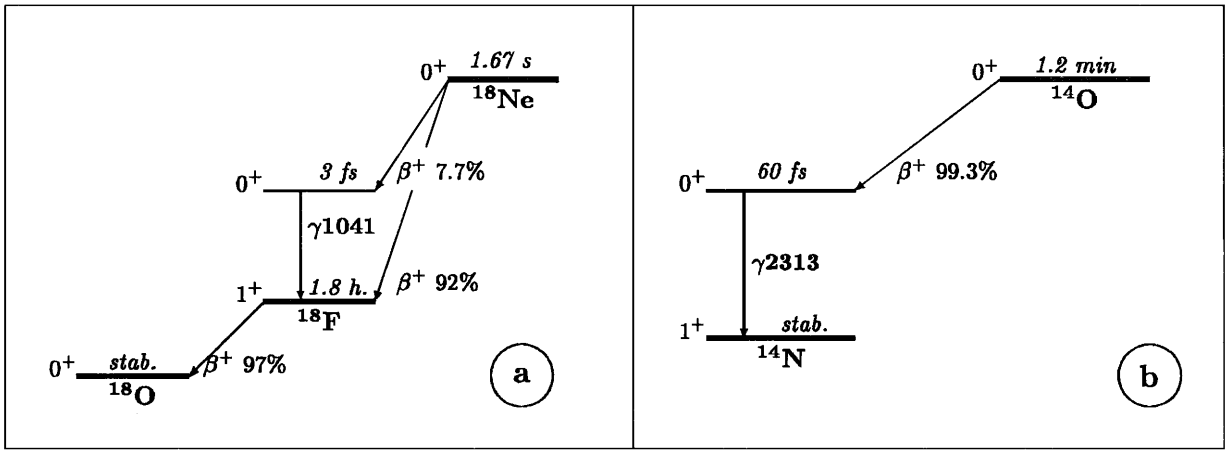

Fig. 4. Relevant parts of the decay schemes of the ^{18}Ne (a) and ^{14}O (b) nuclei.

The function has a minimal value $U_{\min}$ at the point $r = r_{\min}$. The initial values of the parameters $U_{\min}$ and $r_{\min}$ chosen

$$U^0_{\min} = -5.51\,\text{eV}, \qquad r^0_{\min} = 1.192\,\text{Å} \tag{9}$$

correspond to parameters of O-(CO) binding in the former CO_2 molecule. The beta-decay of ^{14}O disturbs the electromagnetic balance of the molecule causing an instantaneous change of the interatomic potential. The parameters of this new interatomic potential are the object of our interest.

In order to test the sensitivity to the different parts of the potential-energy dependence, the parametrisation

$$U(r) = \begin{cases} \lambda_s U_{\text{LJ}}(r) + (\lambda_u - \lambda_s) U_{\min}, & \text{if } r \le r_{\min}, \\ \lambda_u U_{\text{LJ}}(r'), & \text{if } r > r_{\min} \\ \text{with } r' = r_{\min} + \lambda_l (r - r_{\min}) & \end{cases} \tag{10}$$

has been used. The $U_{\text{LJ}}(r)$ is defined in (8). The new dimensionless parameters allowed to vary separately the short- (λ_s), middle- (λ_u) and long-range (λ_l) part of the potential-energy dependence. The short-range part determines the potential depth and steepness, while the parameter λ_l of the long-range part contracts or expands the potential well beyond $r_{\min}$. For $\lambda_s = \lambda_u = \lambda_l = 1$ the formula (10) transforms back to (8).

The simulation of the interatomic perturbation was performed in the following way:

1. the initial momentum of the recoiling ^{14}N nucleus $\mathbf{R}^0$ was taken from the analysis program (this will be discussed later in subsect. 4.2);
2. the ^{14}N-(CO) system was randomly directed relative to $\mathbf{R}^0$ and the initial distance ^{14}N-(CO) was always fixed to $r^0_{\min}$ (eq. (9))[6];
3. the CO and ^{14}N was tracked in the potential chosen ((8) or (10)) until either the emission of the γ-quantum[7] or the breaking of their contact;
4. the ^{14}N momentum obtained, $\mathbf{R}'$, was returned to the analysis program.

3 Experimental procedure

Whereas the beta-decay of ^{18}Ne was measured in our previous experiment [5], the beta-decay of ^{14}O was investigated in this project. The ^{14}O nucleus seemed to be an ideal case due to 99% intensity of the branch of interest (7% for ^{18}Ne) and the potentially lower annihilation radiation background (two *versus* four annihilation gammas per decay), as one can see from fig. 4.

As the half-life of the excited level in ^{14}O is rather long ($\tau = 60\,\text{fs}$), a gaseous target was developed instead of the solid one used previously for the ^{18}Ne ($\tau = 3\,\text{fs}$) measurement.

The experimental setup is shown in fig. 5. A CO-gas target was used at atmospheric pressure. It was continuously recycled. The ^{14}O produced in the irradiation chamber with the ^{3}He beam (12 MeV, 300 nA) of the MP Tandem accelerator (IPN, Orsay), using the ^{12}C(^{3}He, n)^{14}O reaction, was transported by this gas flow to the measuring cell ("bubble" of 5.6–5.9 cc made of a thin mylar foil). A set of devices purified the gas target. Filters captured the solid and chemically active contaminants before the bubble and a cold trap caught the water and other possible admixtures flowing out of the measuring chamber. At the end of a cycle the gas target was kept in a buffer reservoir of 5 l allowing any long-lived radioactive contaminants to decay. The gas was circulating at 6–10 cc/min.

The target materials were selected in a way to minimise the surface absorption of ^{14}O. This effect was tested using an "impulse" operation of the gas target. In this

[6] Contrary to the changes of interatomic potential (parameters $U_{\min}$ and $r_{\min}$ (eq. (8))), the initial ^{14}N-(CO) distance is of course equal to the previous ^{14}O-(CO) one. However, as the potential is modified, the equilibrium position differs in general from the initial one.

[7] The time of γ-quantum emission was randomly chosen according to the exponential de-excitation of the daughter's excited state ($\tau = 60\,\text{fs}$).

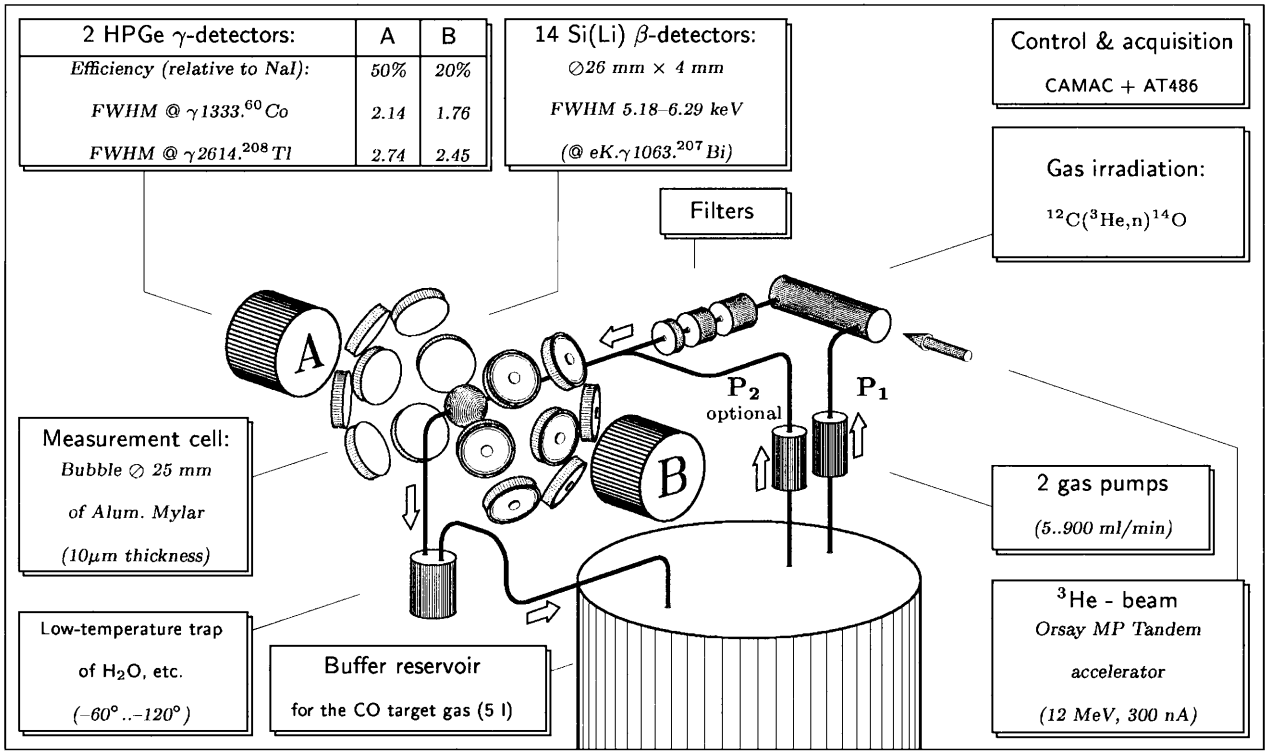

Fig. 5. The layout of the experimental setup to measure beta-neutrino angular correlation in a gaseous target.

mode the pumps (P_1, P_2) were switched cyclically so as to bypass periodically the irradiation chamber (using the pump P_2). The time evolution of the residual ^{14}O activity was measured in phase with the blowing of non-irradiated gas. It was found that the portion of ^{14}O sticking on the surface of the mylar bubble and Teflon feeding tubes did not exceed 10^{-3}.

Many efforts were also made to choose the optimal gas target. For example, the hydrocarbonates (CH_4, C_4H_{10}) were rejected because of significant undesirable reactions[8]. Finally, carbon oxide CO was chosen as the best source transport agent.

The detection system was similar to the one used in the ^{18}Ne experiment (see description in ref. [5] and the current parameters in fig. 5). Positrons were registered with 14 Si(Li) detectors, whereas the coincident gamma-rays were observed with two HPGe detectors A and B. The particle energies E_γ and E_β, the identification number of the fired beta detector and the time interval $T_{\beta\text{-}\gamma}$ between the fast signals of the beta and gamma detectors were stored event by event. The experimental data were accumulated in runs of equal length. The non-coincident single γ-spectra were also stored during a short time (30 s for each detector) at the end of each run (15–40 min). These spectra were used to monitor the stability of the experimental conditions (drift and distortion of spectral peaks) and to determine the energy resolution of the γ detectors. More than 200 runs were collected during one week of measurement. A typical γ-spectrum, β-spectrum and time coincidence curve $T_{\beta\text{-}\gamma}$ are shown in fig. 6. After a preliminary data selection, we obtained $\sim 2 \times 10^6$ events in the γ peak of interest ($E^0_\gamma = 2313$ keV), which were then used for further data analysis.

[8] The products of the beam-induced dissociation (organic radicals) caused polymerization, polluting the whole target system.

4 Data analysis

The data analysis consisted in two parts, which are i) the processing of experimental data; ii) a theoretical simulation and the fit. These procedures are separately presented below.

4.1 Experimental Doppler shift

The analysis of the experimental data is similar to the one, done in the ^{18}Ne experiment. Therefore, we refer the reader to our previous publication [5] and present here only the modifications and the new specific features of the procedure.

- The Doppler shifts were determined separately for groups of runs (192 for detector A and 102 for B) stored at comparable experimental conditions.
- The total beta-spectrum was divided in 20 bins, all with the same amount of statistics.
- Strict ($\sim 75\%$ of the total statistics) and soft ($\sim 95\%$) coincidence time cuts $T_{\beta\text{-}\gamma}$ were probed to select true coincidences. Both choices led to the same final results,

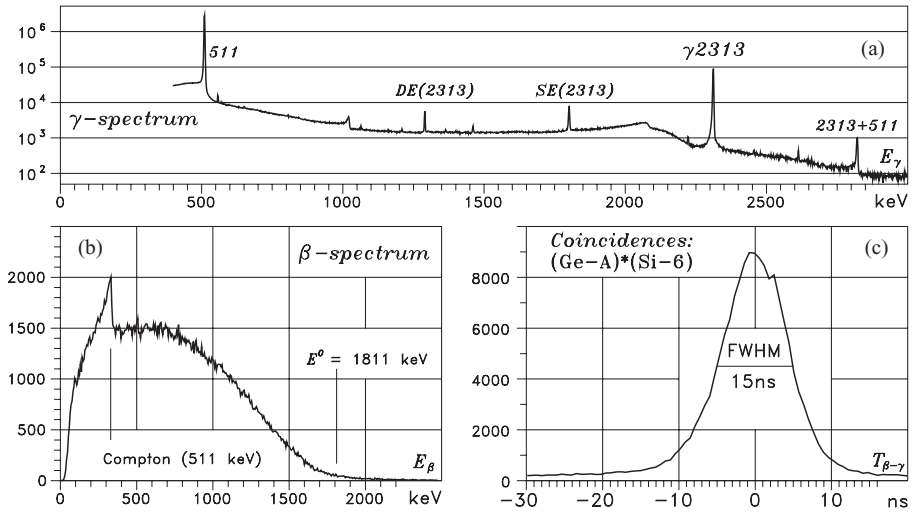

Fig. 6. Examples of experimental gamma- (a) and positron- (b) spectra measured in coincidence. A corresponding coincidence time spectrum is presented in (c).

demonstrating the absence of any systematic error due to this cut.

- The position of the γ detectors was inverted in the middle of the experiment, and both halves of data were processed separately. The similarity of the results obtained indicates the absence of significant systematic error due to the setup geometry.
- For each energy range of the beta-particles (20 bins), for each γ detector (A, B) and for each run, the following procedures were performed:
  - the 2313 keV γ-lines were constructed for each Si-HPGe true coincidences (14 spectra) and were grouped in 7 pairs according to the coincidences of γ detector with two diametrically opposite β detectors. The γ peaks in each such pair are Doppler shifted, as one can see in fig. 7;
  - the experimental Doppler shift $2\delta E_\gamma^{\exp}$ was obtained for each such pair of γ-lines using five different procedures. The difference between the first moments of two γ peaks was calculated in the simplest method, while in other methods simultaneous fits of both γ peaks by Gaussians with a different number of free parameters[9] were performed. It was found that all results obtained were in good agreement with each other, excluding a systematic error connected with the peak analysis. The method producing the smallest error bars was chosen;
- the weighted mean values of $2\delta E_\gamma^{\exp}$ were calculated over all runs for both gamma detectors and all pairs of beta detectors separately. A dividing factor 0.95 was then used for the pair of central beta detectors, while the factor 0.707 was used for the pairs of lateral beta detectors[10].

From the weighted average of these normalized $2\delta E_\gamma^{\exp}$ values, we obtained the average double Doppler shift as a function of the positron energy tabulated for 20 beta energy bins. This experimental curve was then compared with the theoretical ones (see example in fig. 2), the calculation of which is discussed in the next section.

4.2 Theoretical Doppler shift

The simple ideal expression (7) became more complicated in the case of the real setup geometry, where one has to integrate over the solid angles of the real source and of the detectors. One has to control also precisely the behaviour of the positron, which can:

1. deposit the whole energy in a detector;
2. scatter out or pass through a detector leaving only part of its energy;
3. miss a detector and stop outside of it producing an annihilation radiation which Compton-scatters inside the detector[11];
4. hit the detector (cases 1 or 2) and produce an annihilation radiation which Compton-scatters in the same detector (case 3).

Contrary to the first scenario, the three others distort the experimental Doppler-shift curve and, therefore, must be taken into account in Monte Carlo simulations.

The number of coincidences between the 2313 keV gamma-rays and the annihilation radiations observed in the beta detector (scenario 3) is rather large (one can see

[9] The γ-line width, background pedestal and slope were either fixed or free parameters depending whether we assumed their knowledge or not. An important correction due to random coincidences was also included, as is explained in [5].

[10] These factors represent the mean cosine $\langle(\mathbf{p}\cdot\mathbf{k})\rangle$ which have been defined from the simulation of the setup.

[11] Full absorption of annihilation rays is negligible due to the low efficiency of the beta detectors for the gamma-rays.

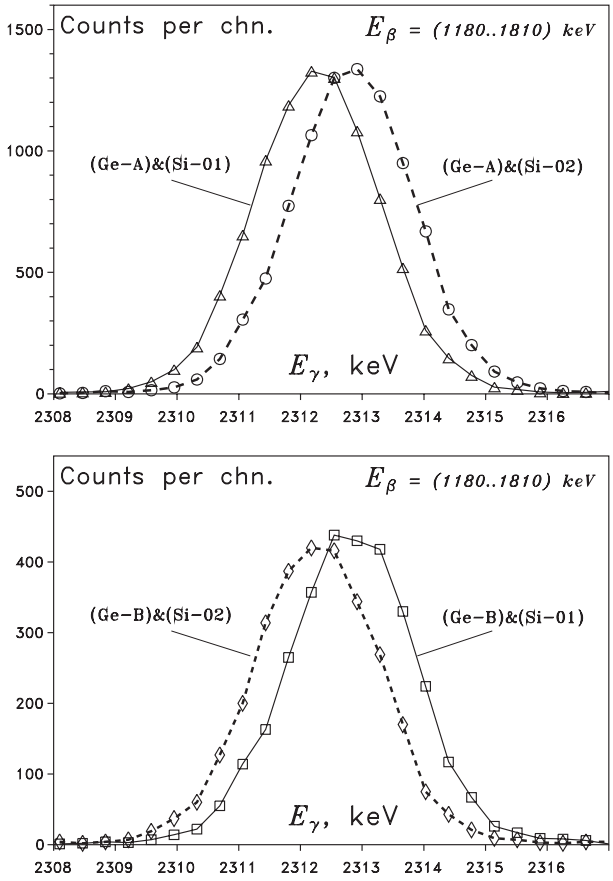

Fig. 7. Typical Doppler shifts of γ-lines measured by each γ detector (Ge-A, Ge-B) in coincidence with high-energy positrons ($>$ 1180 keV) stopped in the axially placed (Si-1, Si-2) β detectors.

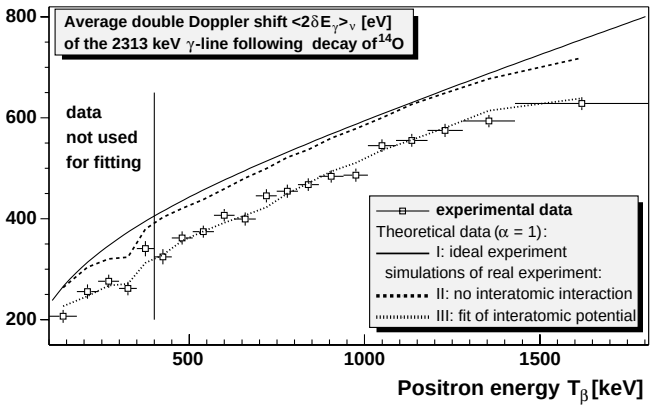

Fig. 8. Theoretical and experimental Doppler-shift curves. Line I corresponds to the ideal setup (eq. (7)), while Line II was obtained for the real one (subsect. 4.2) (no interatomic interactions in both cases). Line III is a best fit assuming interatomic effect (potential (8) with two adjusted parameters $R_{\min}$ and $U_{\min}$) in the real setup. Pure V interaction ($\alpha \equiv 1$) was assumed in each cases.

in fig. 6b the characteristic Compton bump in the low-energy range of the beta-spectrum). In order to exclude completely this systematic effect the low-energy part of the Doppler-shift curve (the first five bins with $\sim 25\%$ of total statistics) was not used.

In order to calculate the Doppler-shift curve including the systematic effects discussed, the experiment was simulated with the GEANT package (version 3.21) of CERNLIB [8]. The reliability of GEANT to track electrons and gammas at the low-energy region (100 keV–10 MeV) was proven in a dedicated test[12].

The calculation of the Doppler-shift curve was performed in two steps.

1. First, the simulation of events in the setup was performed by GEANT. Isotropically emitted positrons with their energies randomly distributed according to the beta-spectrum shape were generated from a random position in the source assuming a homogeneous ^{14}O distribution in the bubble. If only one of the 14 beta detectors[13] was fired by a positron or its annihilation photon, then:
   - the interaction point of the 2313 keV γ-quantum was randomly generated in the HPGe volume assuming an homogeneous distribution of the emitting ^{14}N nuclei in the source volume;
   - the isotropic direction of the neutrino momentum was simulated fixing finally the kinematics of the process;
   - the parameters required to calculate the Doppler-shift curve were stored event by event recording i) the initial momentum of the positron, of the recoiling daughter nucleus and of the neutrino; ii) the energy of the gammas; iii) the energy deposited in the beta detector; iv) the identification number of the fired beta detector.

   About 3×10^6 events were simulated in this way and used in the next step of the analysis.
2. In a second stage, the Doppler shifts were calculated accordingly to eq. (5) for each simulated event. Before this calculation, the momentum of the recoil $\mathbf{R}$ was either corrected or unchanged depending whether the interatomic effect was considered or not (see subsect. 2.2). The values, thus, obtained were then grouped in 20 bins using the same cuts for the energy deposited in the beta detector as in the experimental data analysis. In order to take into account the beta-neutrino angular correlation, each Doppler shift was accumulated with the weight calculated using eq. (1) to evaluate its mean value. The $2\delta E_\gamma$ so computed for pairs of beta detectors are divided by 0.95 and 0.707 as in the analysing procedure (see subsect. 4.1). For the error determination, the number of events in each beta energy bin was used.

[12] The correctness of the simulation of energy losses as well as the angular characteristics of the tracking (*e.g.*, scattering of the particles) were tested.

[13] This corresponds to the experimental hardware trigger, where events are rejected if more than one beta detector was fired.

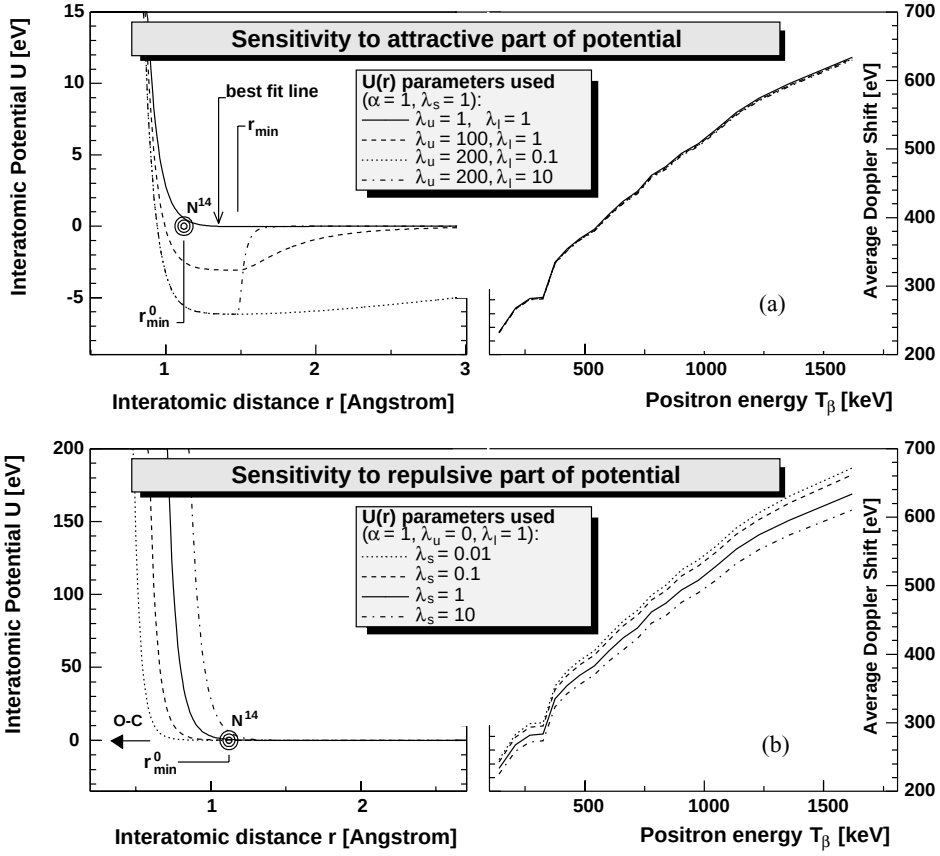

Fig. 9. Sensitivity of the Doppler-shift curve to variations of the attractive (a) and repulsive (b) part of the interatomic potential after beta-decay as a function of the (O-C)-^{14}N distance . Simulations with the shapes of the interatomic potentials displayed on the left side of the pictures result to average Doppler shift *vs.* positron energy dependence shown on the right side (drawn by the same type of line as the corresponding potential). The potential with the shape parameters $\lambda_s = \lambda_u = \lambda_l = 1$ is the one obtained from the fit (eq. (11)) —displayed as the best fit line. The r^0_{min} is the original distance of the ^{14}N from the (O-C) complex (the rest of the former CO_2 molecule); the r_{min} is the parameter used in (10) of the potential after the β-decay.

Whereas the first step was made only once, the second operation was repeated many times changing[14] the correlation coefficient α or the parameters of the interatomic potentials (eqs. (8), (10)). Finally these parameters were optimised to adjust the experimental data.

5 Results

The different theoretical Doppler-shift curves as well as the experimental one are presented in fig. 8. One can see that the experimental Doppler shift is suppressed by 10%–15% in comparison to the theoretical curves corresponding to both ideal and real setups (Lines I and II, respectively in fig. 8). These curves were calculated in the absence of both interatomic interactions and scalar coupling admixture ($\alpha = 1$). Introducing the interatomic effect (subsect. 2.2) and fitting the data with r_{min} and U_{min} parameters of the potential (8), reasonable values were obtained (67% CL):

$$\left.\begin{array}{l} U_{min} = -0.03 \pm 0.01\,\text{eV} \\ r_{min} = 1.48 \quad \pm 0.04\,\text{Å} \end{array}\right\} (\chi^2 = 1.3), \tag{11}$$

indicating excellent agreement between experimental and theoretical data (Line III in fig. 8). This result proved that the reduction of the experimental Doppler-shift curve can be attributed to the interatomic effect. It is also important to emphasize that there is no significant deviation between the first five bins in comparison with the other ones although these points were excluded from the fit due to the observed coincidence of the annihilation rays with the 2313 keV γ-line (see subsect. 4.2); one can conclude that GEANT simulates this effect with success.

Fixing U_{min} and r_{min} given in (11) and performing a fit with α as a free parameter, the statistical sensitivity of our measurement to the correlation coefficient was evaluated (67% CL):

$$\alpha = 1.00 \pm 0.03 \quad (\chi^2 = 1.3), \tag{12}$$

where of course the error is the only meaningful value.

[14] The MINUIT (CERNLIB) package was used for these purposes [9].

The sensitivity of the experiment to different ranges of the interatomic potential was then examined using the potential (10). The Doppler-shift curves were calculated for different sets of λ_i parameters, which influence separately different parts of the interatomic potential. The results are presented in fig. 9. One can see, that the Doppler-shift curve is practically insensitive to the attractive (middle- and long-range) interatomic forces (fig. 9a) and is very sensitive to the repulsive (short-range) part of potential (fig. 9b).

6 Discussion and conclusions

As for the main goal of this experiment, a 3% *statistical* sensitivity to the correlation coefficient α (eq. (12)) could be reached, which corresponds to a sensitivity to the admixture of a scalar coupling at the 10% level, if the interatomic interactions would be known. Unfortunately, it is very difficult to evaluate the *systematic* error introduced by the interatomic effect observed and thus obtain a new improved result for the scalar interaction. New, more realistic (and complicated) models of the interatomic interaction following the beta-decay should be developed and applied instead of the simple one used in the current article. These models must be accurate at the level of several percent in order to contribute only at the level of $\leq 1\%$ in the systematic error of α. This difficult work has still to be done.

Nevertheless, approaching the problem from the opposite side, it was proven that the observed Doppler shift is very sensitive to the interatomic effect (see fig. 8). Thus, inverting the task one can investigate the interatomic interaction in the beta-neutrino angular-correlation assuming the validity of the SM ($\alpha = 1$).

The beta-decaying nucleus can be introduced by different ways (chemistry, off-line and on-line nuclear irradiation, etc.) at a definite site inside the sample, which, in turn, can be in a different state (solid, liquid, or gas)[15]. Measuring the decay kinematics of this marker by the method described in the present article, one can probe the microscopic properties of the sample investigated. This was demonstrated in the frame of a simple Lennard-Jones model (eq. (8)). The parameters $U_{\min}$, $r_{\min}$ of this model were obtained (eq. (11)).

The method proposed provides a rather flexible tool from several points of view. Various beta-decaying isotopes are characterised by different energy constants Q_β, half-lives τ and de-excitation energies E^0_γ of the levels present in the daughter nuclei. Therefore, choosing different tagged atoms one can vary energy and interaction time (distance) of the recoils in the sample. Changing the geometry of the setup one can investigate also the anisotropy of interatomic interactions in the sample (*e.g.*, in the case of crystalline or polarized targets).

It was demonstrated, that our observables are especially sensitive to repulsive (short-range) interatomic forces, which are tested at the energy level of hundreds eV (see fig. 9). We would like to stress that this energy range can hardly be reached by other ways. Indeed, the eV energy region is covered by methods of molecular and solid physics, optics, etc., while the nuclear and ion beam technique is available starting from the keV energy region. Therefore, the method proposed can be considered as a new complementary tool to other well-known methods to study interatomic interactions in matter.

Taking into account the present work, we can conclude that the absence of the interatomic effect is a *necessary requirement* for experiments aiming to search for scalar coupling in beta-neutrino angular correlation. It was therefore decided to repeat the measurement with ^{18}Ne nucleus including several changes. Using a gaseous oxygen target instead of the solid one used previously [5], we will: i) totally exclude the interatomic effect thanks to the chemical inertness of the atom investigated; ii) increase the counting rate due to an effective suppression of the background. This project is now in progress.

This work has been partially supported by grant 96-02-18935 of the Russian Foundation for Fundamental Research. It has been carried out within the IN2P3, CNRS-JINR collaboration agreement 99-44. The authors are very grateful for these supports. We also thank the JINR detector group (V. Sandukovsky, S. Katulina) for the preparation of Si(Li) detectors, A. Kachalkin, A. Salamatin for technical assistance and the staff of the Orsay MP Tandem accelerator for the excellent beam conditions. We also acknowledge A. Cassimi (GANIL) for fruitful discussions.

References

1. E.G. Adelberger *et al.*, Phys. Rev. Lett. **83**, 1299 (1999).
2. C.H. Johnson, F. Pleasonton, T.A. Carlson, Phys. Rev. **132**, 1149 (1963).
3. F. Glück, Nucl. Phys. A **628**, 493 (1998).
4. Yu. Shitov *et al.*, Nucl. Phys. A **699**, 917 (2002).
5. V.G. Egorov *et al.*, Nucl. Phys. A **621**, 745 (1997).
6. W.E. Ormand, B.A. Brown, B.R. Holstein, Phys. Rev. C **40**, 2914 (1989).
7. E.K. Warburton, D.E. Alburger, D.H. Wilkinson, Phys. Rev. C **26**, 1186 (1982).
8. *GEANT —Detector Description and Simulation Tool*, **W5013**, CERN, 1993.
9. F. James, *MINUIT —Function Minimisation and Error Analysis*, **D506**, CERN, 1994-1998.

[15] The only limit is that this sample must be thin enough to allow the beta-particles to escape from it.